

Mechanical properties of Al/Al₂O₃ and Al/B₄C composites

Vinod K. Pandey^{*1}, Badri P. Patel^{2a} and Siddalingappa Guruprasad^{3b}

¹Research and Development Establishment (Engineers), Pune, India

²Applied Mechanics Department, Indian Institute of Technology Delhi, New Delhi, India

³DRDO HQ, New Delhi, India

(Received August 26, 2016, Revised January 9, 2017, Accepted January 13, 2017)

Abstract. Mechanical properties of Al/Al₂O₃ and Al/B₄C composites prepared through powder metallurgy are estimated up to 50% Al₂O₃ and 35% B₄C weight fractions using micromechanics models and experiments. The experimental Young's modulus up to 0.40 weight fraction of ceramic is found to lie closely between Ravichandran's/Hashin-Shtrikman lower/upper bounds, and close to self consistent method/Miller and Lannutti method/modified rule of mixture/fuzzy logic method single value predictions. Measured Poisson's ratio lies between rule of mixture/Ravichandran lower and upper bound/modified Ravichandran upper bounds. Experimental Charpy energy lies between Hopkin-chamis method/equivalent charpy energy/Ravichandran lower limit up to 20%, and close to the reciprocal rule of mixture for higher Al₂O₃ content. Rockwell hardness (RB) and Micro-hardness of Al/Al₂O₃ are closer to modified rule of mixture predictions.

Keywords: mechanical properties; hardness; micro-mechanics; powder processing; functionally graded material

1. Introduction

Functionally graded materials (FGMs) are the advanced materials in the family of engineering composites made of two or more constituent phases with continuous and smoothly varying composition usually in thickness direction to reduce in-plane and through-the thickness transverse shear stresses, thermo-elastic property mismatch and to improve bi-material bonding, mechanical integrity and fracture toughness as compared to bi-materials. FGMs can be fabricated by mixing ceramic and metal or any combination of different metals using various techniques such as physical vapor deposition, chemical vapor deposition, plasma spraying method, infiltration techniques, powder metallurgy, solid free form, selective processing, buoyancy-assisted casting and diffusion etc. In the present study, powder metallurgy (PM) technique is used to fabricate Al/Al₂O₃ and Al/B₄C FGMs due to its superior performance for making metal/ceramic FGMs and cost effectiveness. Al has compatibility with other materials for instance, Aluminium is added with lower density material Mg (Mahendran *et al.* 2012), with Ti to form TiAl (Kothari *et al.* 2012),

*Corresponding author, Professor, E-mail: vinu2pme@gmail.com

^aMTech. Student

^bPh. D.

with Ni (Srivatsan *et al.* 2012). Alumina has compatibility with materials such as NiAl having higher density (Chmielewski *et al.* 2014). Composites and FGMs of Al/Al₂O₃ have advantage of complete thermodynamic compatibility and don't exhibit solubility of one phase to another resulting in strong interfacial bonding (Dalglish *et al.* 1998). They are widely used for high performance applications such as automotive, military (Ezatpour *et al.* 2013), aerospace, engineering structures, geotechnical sector (Chegenizadeh *et al.* 2014), Aerospace engines, computer circuit boards, re-entry vehicles, nuclear components and other engineering application due to improved physical and mechanical properties.

FGM properties can be obtained using: (i) Theoretical models in which mechanical properties vary exponentially or linearly or logarithmic or power law with position, (ii) Micromechanics techniques, (iii) Experimental techniques in which variation of properties may be determined by testing of Non-FGM specimens with a range of compositions. Many micromechanics techniques are available in the literature to predict the elastic constants of composites and functionally graded materials (Sajjadi *et al.* 2013). These techniques can be divided into two categories namely, the one predicting upper and lower bounds such as Ravichandran's bounds (Hsieh *et al.* 2004, Hsieh and Tuan 2005, 2006, Ravichandran *et al.* 1994), Modified unit cell model (Hsieh and Tuan 2005) and Hashin-Shtrikman (H-S) bounds (Joseph 1995, Hashin *et al.* 1963, Zimmerman 1992, Hsieh *et al.* 2005). Subsequently, H-S bound was modified to include the effect of microstructure and interconnectivity of the phases at the interface by modifying volume fraction to be of exponential form for bulk modulus, while for shear modulus, it appears as nonlinear third order form (Upadhyay *et al.* 2012) The techniques which predict single values of the elastic properties of two-phase materials such as Self consistent model (SCM) (Joseph 1995, Hill 1965), Modified rule of mixture (MROM) (Tamura *et al.* 1973, Kapuria *et al.* 2008), Mori Tanaka Method (MTM), (Budiansky 1965, Mori and Tanaka 1973), Wakashima and Tsukamoto (WTM), (Budiansky 1987), Kerner method (KM) (Joseph 1995, Wakashima and Tsukamoto 1990), Fuzzy Logic Method (FLM) (Sasaki *et al.* 1989, Hirano *et al.* 1990), Miller and Lannutti method (MLM) (Hirano *et al.* 1991, Miller *et al.* 1993), Hopkin-Chamis method (HCM) (Gibson 1994), and Coherent Potential Approximation (CPA) (Nan *et al.* 1993) etc. Kim and Muliana 2010 studied rate independent and inelastic behaviour for hybrid composites using combined Schapery's viscoelastic integral model and Valenis's endochronic viscoplastic model. Subsequently, Kim *et al.* (2011) used multiscale approach to predict the elastic properties of nanoparticle reinforced polymer composite using the ensemble-volume average method and the MD simulation. Phabhu *et al.* (2015) studied synergistic effect of clay and polypropylene based ternary hybrid composite.

The comparison of micromechanics predictions with experiments for a range of functionally graded materials is limited. Rousseau and Tippur (2002) studied variation of elastic properties of A-glass/Epoxy FGM samples up to 52% volume fraction of A-glass fabricated using gravity casting technique. The Young's modulus and Poisson's ratio, measured using ultrasonic pulse-echo and beam deflection methods, were closer to Mori-Tanaka method (MTM) (Joseph 1995, Budiansky 1965, Mori and Tanaka 1973) compared to Halpin-Tsai micromechanics techniques. Tilbrook *et al.* (2005) used reciprocal rule of mixture (RROM), H-S bounds, Tuchinskii unit cell upper and lower bounds and effective medium approximation (EMA) micromechanics approaches to compare with the elastic properties measured using Impulse excitation technique for Alumina-Epoxy FGM samples for epoxy volume fraction varying from 5 to 50% and was found that the Young's modulus increases with the percentage of Alumina and EMA technique predicted the elastic properties of the two phase composite with interpenetrating network accurately.

Castro *et al.* (2002) studied the variation of Young's modulus measured using tensile test as per

ASTM-E-8 of A359/SiC_p composite fabricated using centrifugal casting and compared the measured values with the Self Consistent Method (SCM) for full volume fraction range. It was shown that the Young's modulus and Rockwell hardness increase with the increase in SiC_p volume fraction as expected. Atri *et al.* (1999) evaluated the elastic properties of Ti, TiB and TiB₂ composite samples using Impulse excitation technique. The experimental values of Young's modulus for different volume fractions of TiB were found to lie between Voigt and Reuss bound but deviated from those predicted using Halpin-Tsai (HT) and Hopkins-Chamis (HC) methods. The variation of Poisson's ratio closely followed the rule of mixture prediction.

The elastic properties of Al₂O₃-NiAl for NiAl volume fraction from 0 to 100%, SiC-Al composite up to 74% SiC volume fraction, Glass-W systems in the range of 50-90% of glass and WC-Co system for Co from 50-98% composite samples fabricated using powder metallurgy were measured using ultrasonic technique by Hsieh *et al.* (2004), Hsieh and Tuan (2005), Hsieh *et al.* (2006) and were found to be within Voigt -Reuss bounds and closer to H-S lower bound. Gaharwar and Umashankar (2014) and Ezatpour *et al.* (2013) fabricated Al/Al₂O₃ composites of 3, 5, 7 and 10% Al₂O₃ volume fraction using powder metallurgy and stir casting process, respectively, and experimentally evaluated density, electrical conductivity, strength and hardness.

It can be concluded from the above literature review that the mechanical properties of a number of MMCs were evaluated experimentally and compared with the micromechanics predictions. However, the studies on Al/Al₂O₃ and Al/B₄C composites are limited up to 10 % weight fraction of ceramic, and further, there are no comparative studies of experimental and predicted elastic properties of these composites. Al/Al₂O₃ and Al/B₄C composites are widely used for high performance applications such as automotive, military (armour plate and bullet proof jackets), aerospace and electricity industries due to their high specific strength/stiffness, wear and environmental resistance. The study on Al/Al₂O₃ and Al/B₄C composites gains greater importance since the melting points of aluminium (670°C), alumina (2050°C) and boron carbide (2150°C) are significantly different and pose challenge for fabrication of Al/Al₂O₃ and Al/B₄C composites.

In this study, the fabrication and the estimation of the mechanical properties of Al/Al₂O₃ and Al/B₄C composite samples prepared through powder metallurgy technique are extended beyond 10% Al₂O₃ i.e., up to 50% Al₂O₃ and 35% B₄C respectively using different micromechanics models and are compared with the experimental results. Young's modulus of the composite samples is measured using impulse excitation technique and compared for both bound based techniques and single value based prediction techniques. Stress to strain transfer factors for both materials are evaluated which are required to predict properties using Modified rule of Mixture. Hardness and Charpy impact energy of the composite samples are also measured and compared with the micromechanics predictions using rule of mixture, reciprocal rule of mixture, modified rule of mixture, Ravichandran's lower/upper bounds and Hopkin Chamis Method by replacing Young's modulus with hardness or Charpy impact energy. The Equivalent Charpy Energy (CEQ) and Equivalent Hardness (HEQ) are calculated as

$$M = \frac{V_1 E_1 M_1 + V_2 E_2 M_2}{V_1 E_1 + V_2 E_2} \quad (1)$$

Where M is Charpy Impact Energy or Hardness, E_1 and E_2 are elastic modulus of phase 1 and 2, V_1 and V_2 are volume fractions of phase 1 and 2.

2. Experimental procedure

Al/Al₂O₃ and Al/B₄C FGMs and Non-FGMs samples are fabricated using powder metallurgy technique. Commercial 1000 series-aluminium powder (grade 1160) of 99.60% purity and having 15-30 micron particle size and alumina of 99.9% purity powder were mixed for 6 hours in Vibration ball mill with steel balls of 8 mm diameter at 60 rpm including 2% paraffin (to improve bondage) in weight ratios varying from 0 to 50% of Al₂O₃ with increment of 5%. Similarly, Al/B₄C grade 400 SG powder mixtures are prepared in weight ratios varying from 0 to 35% of B₄C. The weight fraction of B₄C is limited to 35% since the sintering temperature used (600°C, bound by the melting temperature of Aluminum) is not sufficient to bond Al/B₄C particles strongly beyond 35% weight of B₄C leading to the decrease in the stiffness and strength properties. The mixed powder composition is used to form non-graded or layered graded compositions in square steel die having inner and outer dimensions of 113 mm×113 mm and 151 mm×151 mm, respectively, and 70 mm height. The powder compacts were pressed up to 50 MPa at room temperature. Initial values of sintering time, pressure and temperature are selected from literature and optimised subsequently. The specimens (100% Al) compacted at various combinations of temperature (500°C to 650°C), pressure (200 bar to 400 bar) and duration (0.5 to 2 hours) were tested for density and Young's modulus. The sintering temperature of 600°C and pressure of 300 bar for 1.5 hours duration resulted in dense samples with Young's modulus equal to 72 GPa. These parameters are used for sintering of other Non-FGM and FGM samples. Eleven different non-FGMs and one FGM for each composition of powders were fabricated in the form of cuboids with 70 mm length, 10 mm height and 5 mm width. The density of Non-FGM and FGM samples is estimated based on measurement of weight/volume and using Archimedes principle. The elastic properties of prepared Non-FGM samples are measured using impulse excitation technique and DEPA data processing software (version-9) from M/s Jagdish Electronics, Bangalore (India). The schematic of the measurement system is shown in Fig. 1. Resonant frequencies were obtained corresponding to flexural and torsional modes, from which Young's and shear moduli, respectively can be obtained. Samples were tested as beams (70 mm×10 mm×5 mm) for Young's modulus and as plates (70 mm×30 mm×5 mm) for modulus of rigidity as per ASTM- C- 1259-08 standard. The instrument is firstly calibrated with calibration block with known Young's modulus provided with the instrument. Three specimens of each Non-FGM are tested and mean and range of property values are reported. The measurements were repeated for each specimen until five consecutive readings of frequency within 1% of variation are obtained.

2.1 Specimen characterization

The samples prepared are used for characterisation tests as follows:

- (i) Density measurement and microstructure study,
- (ii) Determination of Young's modulus and Poisson's ratio,
- (iii) Rockwell and Micro-hardness,
- (iv) Charpy Impact Energy.

2.1.1 Density and porosity

The density of Non-FGM and FGM samples is estimated based on measurement of weight/volume and using Archimedes principle. The theoretical density can be computed for different compositions as

$$\frac{1}{\rho_t} = \frac{W_1}{\rho_1} + \frac{W_2}{\rho_2} \quad (2)$$

Where, W_1 , ρ_1 and W_2 , ρ_2 are weight fraction and density of phase 1 and 2 respectively and ρ_t is

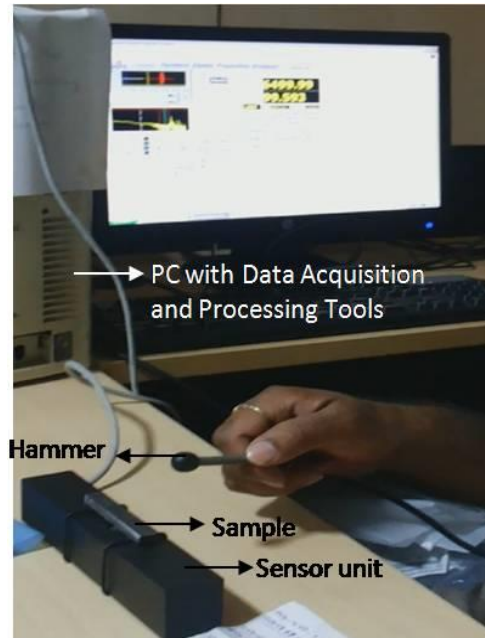


Fig. 1 Setup for measurement of elastic properties

the density of composite.

2.1.2 Microstructural analysis

Optical microscopy on the polished surfaces is used to characterise the aluminium/alumina and to quantify the porosity. Images were obtained using a Nikon 200 microscope and digital camera. The surface to be investigated for each sample is cloth polished with 1- μm diamond paste preceded by standard metallographic preparations. The Non-FGM samples were itched with etchant consisting of Nitric and Hydrochloric acids.

2.1.3 Microhardness

SHIMAZU make microhardness tester with digital display is used to measure microhardness of each layer of Al/Al₂O₃ and Al/B₄C at approximately 0.5 mm distance from 100% Aluminium. The samples are firstly polished with the help of different grade papers with the final polishing direction along axial direction. An indentation load of 0.50 kg for 15 seconds was applied on the FGM samples. The microhardness in the FGM specimens is measured at the centres of the individual layers as well as at the interface. Three measurements are taken at different locations along length of the samples one each at the ends and one at the middle. It is observed that the applied load during the testing did not produce any sign of cracking.

2.1.4 Charpy impact energy

The Charpy impact energy of Al/Al₂O₃ samples is measured with the help of Impact testing machine. The Non-FGM samples of size 55 mm×10 mm×10 mm and different compositions are prepared and tested as per ASTM-E-23 and ASTM-B-925. It is ensured that the striking direction is 90 degrees to the original compact direction for un-notched samples. For notched samples, there

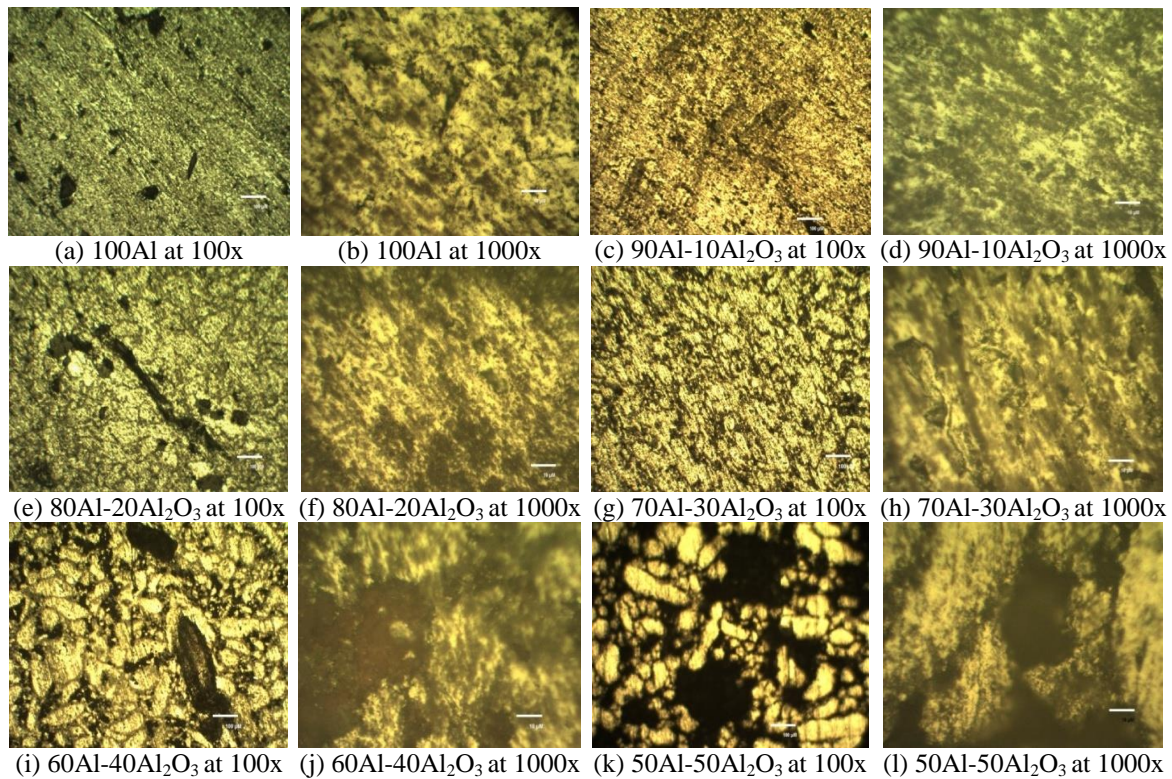


Fig. 2 Microstructure of Non-FGM samples

is no such requirement as per ASTM-E-23. The size of the notched and un-notched samples is taken as per ASTM-E-23 and ASTM-B 925.

3. Results and discussion

3.1 Physical properties-microstructure, density and porosity

Total eleven different compositions of Non-FGMs from 100% Al to 50% Al by weight in steps of 5% reduction of Al with proportionate increase of ceramic and three FGM samples having eleven layers with top layer of 100% Al and bottom layer 50% Al and 50% Al_2O_3 are prepared. The microstructure study is carried out to investigate the distribution of metal/ceramic phases and voids in both FGM and Non-FGM samples. The microstructure for different compositions of Al/ Al_2O_3 Non-FGM samples is shown in Fig. 2 for 100 and 1000 magnifications. These microstructures clearly show the spherical shape of the particles after sintering and uniform distribution of the Al_2O_3 in Al Matrix with minimal clustering/agglomeration for Al_2O_3 less than 30%. It can also be observed from the figure that there are evenly distributed voids in 90/10 Al/ Al_2O_3 Non-FGM sample whereas in 80/20 Al/ Al_2O_3 , voids are concentrated along an oblique line (Fig. 2(c)). The Al_2O_3 particles are separated in the 90/10 Al/ Al_2O_3 and 80/20 Al/ Al_2O_3 Non-FGM samples. Further, 70/30 Al/ Al_2O_3 depicts relatively less void volume fraction. The

Table 1 Density in g/cm³ of Al/Al₂O₃ and Al/B₄C with ceramic weight fraction

Ceramic weight fraction	Al/Al ₂ O ₃		Al/B ₄ C	
	Theoretical (ρ_t)	Experimental (ρ_s)	Theoretical (ρ_t)	Experimental (ρ_s)
0	2.73	2.73	2.73	2.73
0.05	2.77	2.77	2.72	2.71
0.10	2.82	2.80	2.71	2.69
0.15	2.86	2.83	2.69	2.67
0.20	2.91	2.88	2.68	2.66
0.25	2.96	2.93	2.67	2.63
0.30	3.01	2.97	2.66	2.62
0.35	3.06	3.01	2.65	2.60
0.40	3.11	3.05	-	-
0.45	3.17	3.11	-	-
0.50	3.23	3.18	-	-

microstructure of 60/40 Al/Al₂O₃ (Fig. 2(i) and (j)) shows significant void content. The Al₂O₃ particles are continuous phases (interpenetrating network) within the 70/30, 60/40, and 50/50 Al/Al₂O₃ Non-FGM samples depicting weak bonding between them as was also observed by Ezatpour *et al.* (2013). The same is confirmed by measuring the electrical resistivity of the composites as only one phase is good electrical conductor in Al/Al₂O₃ system. Thus, the microstructure of the Non-FGM samples with Al₂O₃ weight fraction in the range 30-50 depicts three-dimensional interpenetrating structure increasing with the increase in Al₂O₃ weight fraction. The variations of theoretical and measured densities with weight fraction of Al₂O₃ and B₄C are given in Table 1. The density of 100% Al samples is measured to be 2.73 g/cm³ using Archimedes principle and weight/volume measurements. The density of Al₂O₃, calculated from density of 95/5 Al/Al₂O₃ sample using Eq. (2), is found to be 3.944 g/cm³ which is close to 3.95 g/cm³ reported by Ezatpour *et al.* 2013. Similarly, the density of B₄C, calculated from density of 95/5 Al/B₄C sample using Eq. (2), is found to be 2.508 g/cm³ which is close to 2.51 g/cm³ reported by Cannillo *et al.* (2006).

The density of the Non-FGM samples increases with the weight fraction of Al₂O₃ and decreases with the weight fraction of B₄C. The porosity ($1 - \frac{\rho_s}{\rho_t}$) calculated from data of Table 2 increases with the addition of Al₂O₃/B₄C due the processing temperature being on the lower side to form bond between Al₂O₃/B₄C during sintering, low wettability, agglomeration and pore nucleation at the Al/Al₂O₃, Al /B₄C interfaces. However, the maximum porosity is less than 2% indicating the good quality of samples.

3.2 Elastic properties of Al/Al₂O₃ and Al/B₄C Non-FGMs

Young's modulus and Poisson's ratio of Al/Al₂O₃ and Al/B₄C Non-FGM samples are determined using impulse excitation technique (IET). Young's modulus values evaluated by striking the sample in two mutually perpendicular directions (one along width and the other along thickness) are found to be nearly same depicting the cross-sectional homogeneity of Non-FGM samples. The comparison of experimentally measured Young's modulus with micro-mechanics

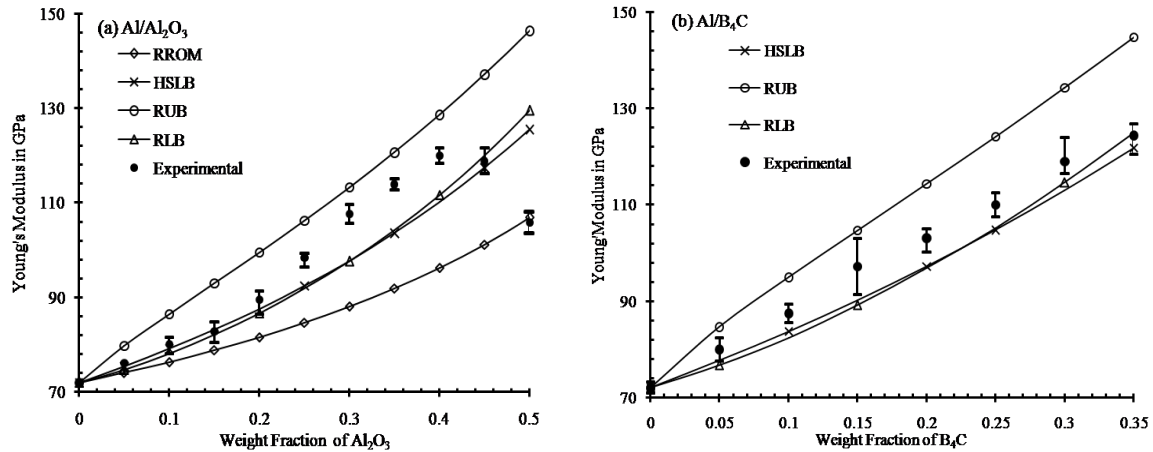


Fig. 3 Comparison of experimentally determined Young's modulus with micromechanics bounds for different ceramic weight fractions: (a) Al/Al₂O₃ (b) Al/B₄C Non-FGM samples

bounds is given in Fig. 3 and single value predictions are reported in Table 2 for Non-FGM samples. In Fig. 3, the micromechanics predictions closest to experimental results only are plotted.

For MROM, the average values of stress to strain transfer factor (q) for Al/Al₂O₃ and Al/B₄C are calculated using the approach given in Joseph 1995, Budiansky 1965 and Mori and Tanaka 1973 from the experimental values of Young's modulus corresponding to 5, 10 and 15% of Al₂O₃ in Al/Al₂O₃ samples (Table 3), taking Young's Modulus of Al₂O₃ and B₄C as 356 GPa (Cannillo *et al.* 2006) and 400 GPa, (Domnich *et al.* 2011) respectively. For a variation of Al₂O₃/B₄C content from 5 to 15%, the change in q is less than 2% even though the effective modulus changes by 18%. Thus, the value of q is less sensitive to the volume fractions of the constituents and the average value of q for the Al/Al₂O₃ and Al/B₄C systems is calculated as 104.5 GPa and 158.43 GPa.

It can be inferred from Fig. 3 and Table 2 that Young's modulus increases from 72 GPa to 119.1 GPa with increase in Alumina from 0 to 40% in Al/Al₂O₃ samples and from 72 to 123.2 GPa with the increase in Boron carbide from 0 to 35% in Al/B₄C samples. The decrease in the experimental Young's modulus beyond 40% weight fraction of Al₂O₃ may be attributed to the fact that the sintering temperature used (600°C) is not sufficient to bond Al/Al₂O₃ particles strongly beyond 40% weight fraction of Al₂O₃. It can also be inferred that the increase in Young's modulus is quite significant compared to the increase in density for Al/Al₂O₃. Both the composites have high specific stiffness even better for Al/B₄C as density decreases with the weight fraction of B₄C and stiffness increases considerably. For Al/Al₂O₃ composite samples up to 0.40 weight fraction of ceramic, the experimental values of Young's modulus are found to lie closely between Ravichandran's/Hashin-Shtrikman lower and Ravichandran's upper bound. Further, the experimental values are close to RLB up to 0.20 weight fraction of Al₂O₃ and up to 0.35 weight fraction of B₄C. The closer prediction of Ravichandran's bound is attributed to its microstructure dependent unit cell comprising of continuous matrix (Al) and reinforcement particles (Al₂O₃ or B₄C) with distinct properties ($E_{Al_2O_3}/E_{Al}=4.94$, $E_{B_4C}/E_{Al}=5.55$). Single value prediction of self-consistent/Miller-Lannutti methods throughout Al₂O₃ weight fraction considered and modified rule of mixture/fuzzy logic method up to 0.25 Al₂O₃ weight fractions are found closer to experimental

Table 2 Comparison of experimentally measured Poisson's ratio and micromechanics predictions

(a) Al/Al ₂ O ₃												
Wt fraction (Al ₂ O ₃)		0.000	0.050	0.100	0.150	0.200	0.250	0.300	0.350	0.400	0.450	0.500
Experimental		0.250	0.251	0.252	0.254	0.255	0.257	0.259	0.261	0.263	0.266	0.268
Micromechanics model	ROM ^a	0.250	0.252	0.254	0.255	0.257	0.259	0.261	0.264	0.266	0.268	0.270
	RLB ^b	0.250	0.250	0.251	0.252	0.253	0.253	0.255	0.256	0.257	0.258	0.260
	RUB ^b	0.250	0.251	0.253	0.254	0.255	0.256	0.257	0.259	0.260	0.261	0.263
	ZLB ^c	0.250	0.243	0.237	0.231	0.226	0.221	0.218	0.215	0.212	0.211	0.211
	ZUB ^c	0.250	0.259	0.268	0.277	0.285	0.293	0.300	0.307	0.314	0.320	0.326
	MRUB ^d	0.250	0.250	0.251	0.251	0.252	0.253	0.254	0.255	0.256	0.257	0.258
	MRLB ^d	0.250	0.230	0.221	0.214	0.209	0.205	0.202	0.199	0.197	0.196	0.196
(b) Al/B ₄ C												
Wt fraction (B ₄ C)		0.000	0.050	0.100	0.150	0.200	0.250	0.300	0.350			
Experimental		0.250	0.2472	0.243	0.240	0.239	0.236	0.234	0.225			
Micromechanics model	ROM ^a	0.250	0.249	0.248	0.247	0.246	0.245	0.244	0.244	0.242		
	RLB ^b	0.250	0.248	0.247	0.245	0.244	0.242	0.241	0.239			
	RUB ^b	0.250	0.233	0.218	0.206	0.195	0.186	0.178	0.172			
	ZLB ^c	0.250	0.254	0.257	0.259	0.261	0.262	0.262	0.261			
	ZUB ^c	0.250	0.247	0.245	0.242	0.239	0.237	0.234	0.232			
	MRUB ^d	0.250	0.249	0.249	0.248	0.247	0.246	0.245	0.243			
	MRLB ^d	0.250	0.224	0.210	0.200	0.191	0.184	0.179	0.174			

^aVoigt (1989); ^bHsieh *et al.* (2004), Hsieh and Tuan (2005, 2006), Ravichandran *et al.* (1994); ^cZimmerman (1992); ^dHsieh and Tuan (2005, 2006)

Table 4 Experimentally measured percentage elongation for different Al₂O₃ weight fractions in Al/Al₂O₃ non-FGM samples

Weight Fraction of Al ₂ O ₃	0.00	0.10	0.15	0.20	0.40	0.50
% Elongation	31.73	22.22	13.15	7.66	4.99	1.40
% Reduction in Ductility	-	29.97	58.56	75.86	84.27	95.59

Young's modulus. HCM predicts the lowest and MLM the highest values of Young's modulus for Al/Al₂O₃ composite. The measured and predicted values of Young's modulus are closer to Modified rule of mixture, Self consistent method and Fuzzy logic method based single value predictions for 0.20 weight fraction of B₄C and FLM from 0.25-0.35 weight fraction of B₄C.

The accuracy of MROM is attributed to the use of stress to strain transfer factor parameter determined from the experimental value of Young's modulus. In SCM, it is assumed that the spherical inclusion (reinforcement) is embedded in concentric spherical annulus of the matrix which in turn is embedded in an infinite medium possessing the unknown effective properties simulating the microstructure observed in the present study. In both Al/Al₂O₃ and Al/B₄C composites, the upper and lower bound predictions through ROM and RROM not reported in Fig. 3, respectively, are farthest compared to experimental values. The significant differences between some of the micromechanics model predictions and experimental results may be attributed to

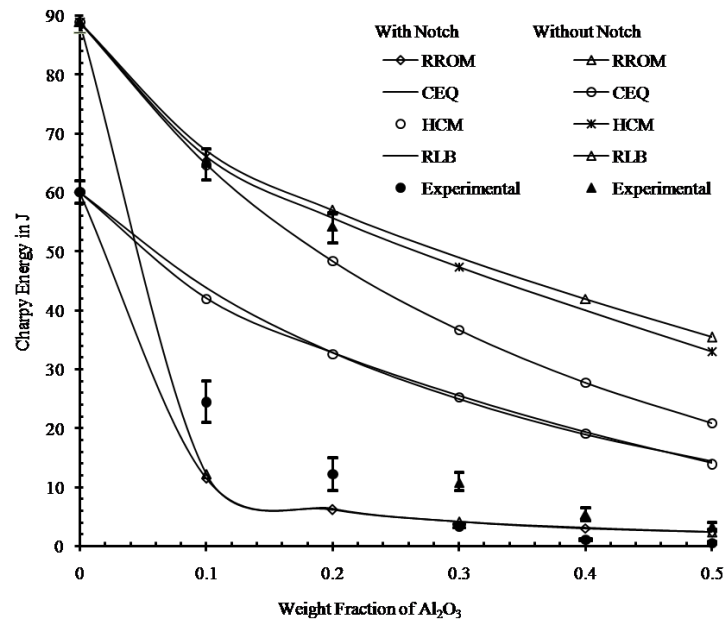


Fig. 3 Variation of Charpy Impact Energy of Al/Al₂O₃ Non-FGM samples with weight fraction of Al₂O₃

model assumptions such as perfect bonding and/or spherical particles shape not met in the prepared composite samples.

The comparison of experimentally measured Poisson's ratio with micro-mechanics bounds is given in Table 3 for Non-FGM samples. The experimentally measured Poisson's ratio is found to lie closely between ROM, RLM, RUB, MRUB for Al/Al₂O₃ system and close to ROM, RLB, ZUB, MRUB for Al/B₄C. For both Al/Al₂O₃ and Al/B₄C composites, predicted values of Poisson's ratio using ZUB/ZLB and MRLB are the found to be farthest as compared to the mean experimental results. It can also be seen from Table 3 that the Poisson's ratio increases with the weight fraction of Al₂O₃ and decreases with the weight fraction of B₄C.

Addition of ceramics e.g., Al₂O₃ decreases the ductility of Al as given in Table 4. The table shows the variation of percentage elongation of Al/Al₂O₃ samples (ASTM-E8) with increase in the weight fraction of Al₂O₃. The decrease in the ductility may be attributed to the introduction of hard phase (Al₂O₃) leading to the hindrance in the dislocation movement.

3.3 Charpy impact energy of Al/Al₂O₃ non-FGMs

Charpy impact energy of Al/Al₂O₃ Non-FGM notched and un-notched samples are determined using Impact tester as per ASTM-E23 and ASTM-B 925. The experimentally measured values are compared with micro-mechanics predictions through reciprocal rule of mixture, Equivalent Charpy energy, Hopkin-Chamis Method (HCM) and Ravichandran's lower bound as shown in Fig. 4. It can be observed from Fig. 4 that the Charpy energy decreases from 89 J to 3.25 J and 60.16 J to 0.50 J from 0 to 50% weight fraction of Al₂O₃ in Al/Al₂O₃ samples for un-notched and notched samples, respectively. For micromechanics predictions, the Charpy impact energy value of notched and un-notched Al samples is taken as 89 J and 60.16 J, respectively, and for Al₂O₃,

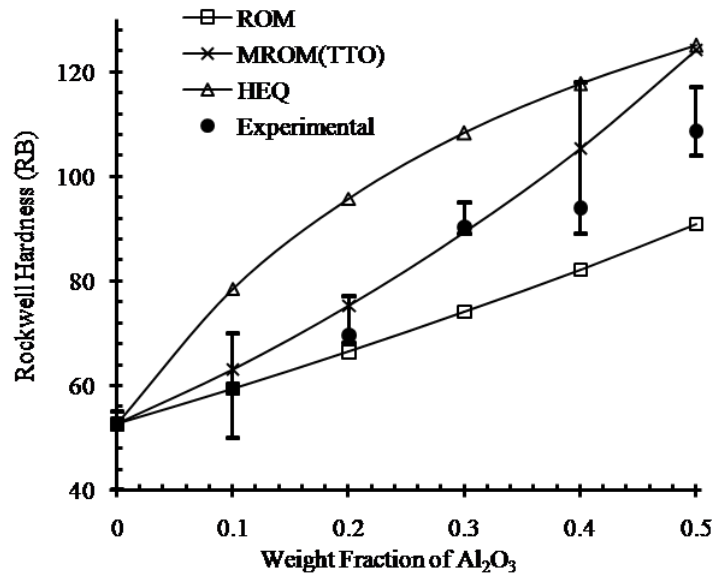


Fig. 4 Variation of Rockwell Hardness of Al/Al₂O₃ Non-FGM samples with weight fraction of Al₂O₃

Charpy value of 1 J is taken for both notched and un-notched samples. The Charpy energy is quite low for Al₂O₃ weight fraction of 0.30, 0.4 and 0.5 compared to that for 0.0, 0.1 and 0.2 weight fractions. The experimental values of Charpy energy are within the wider ROM and RROM micromechanics bounds for Al/Al₂O₃ Non-FGM samples up to 0.50 weight fraction of ceramic. The experimental values of Charpy energy of samples without notch are found to lie closely between HCM, equivalent Charpy (CEQ) and RLB up to 20%, and close to RROM for greater than 20% weight fraction (Al₂O₃) with the experimental values being greater than the RROM predictions. Insufficient sintering temperature for alumina is the main reason for low Charpy energy for the higher weight fraction of Al₂O₃ as the bonding does not take place properly. Ezatpour *et al.* (2013). For notched specimen, the experimental Charpy energy is close to RROM prediction for all Al₂O₃ weight fraction samples tested with the former greater than the latter up to 0.3 weight fraction of Al₂O₃. As compared to the experimental values, the predicted values of Charpy energy equivalent are the farthest on the upper side for both with and without notch cases.

3.4 Hardness of Al/Al₂O₃ non-FGMs

Rockwell hardness of Al/Al₂O₃ Non-FGM samples is determined using Rockwell hardness testing machine (Model-TRS, Make-M/s Fine Testing Machines, Pune, India). The comparison of measured Rockwell Hardness (RB) and that predicted using micromechanics models (rule of mixture, Modified rule of mixture (MROM) also called TTO model, Equivalent Hardness) with weight fractions of Al₂O₃ is shown in Fig. 5. The hardness of 100% Al sample is measured to be 52.66 R_B using Rockwell test machine with 10 kg as minor load and 100 kg as major load. The hardness of Al₂O₃, calculated from hardness of 90/10 Al/Al₂O₃ sample using rule of mixture (ROM), is found to be 146.22 R_B. It is observed that Rockwell hardness increases from 52.66 R_B to 109 R_B for increase in Al₂O₃ weight fraction from 0 to 50%. The experimental values of

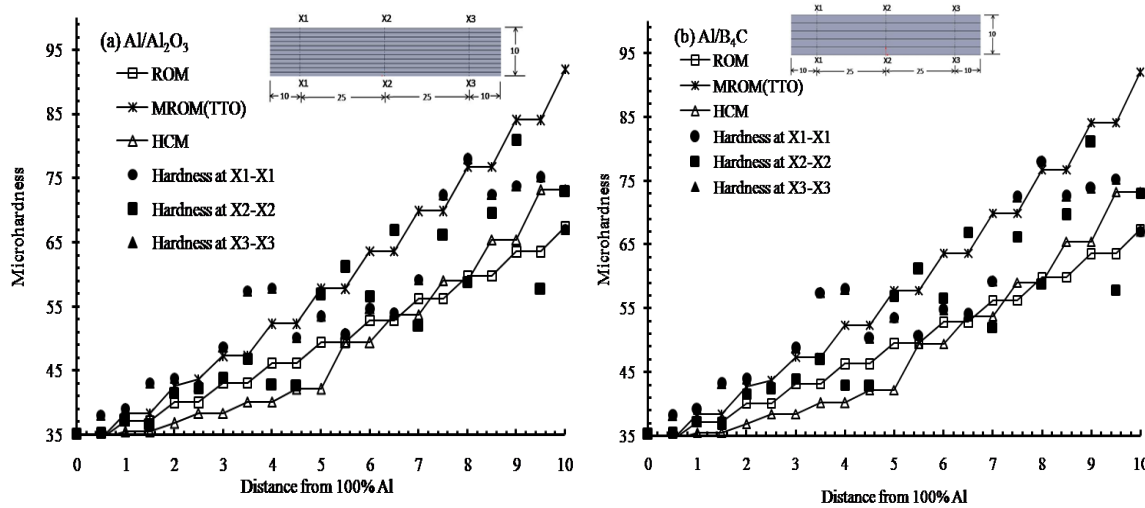


Fig. 5 Comparison of experimental Microhardness with micromechanics bounds along the gradation direction: (a) Al/Al₂O₃ (b) Al/B₄C FGM samples

hardness are within the ROM and HEQ bounds and are close to MROM (TTO) model which is greater than the ROM prediction. It is also observed that Non FGM samples show maximum and minimum variation in hardness corresponding to 0.4 and 0.3 weight fraction of Al₂O₃.

3.5 Micro-hardness of Al/Al₂O₃ and Al/B₄C FGMs

Microhardness tester is used to measure microhardness of each layer of Al/Al₂O₃ FGM starting at approximately 0.5 mm distance from 100% Aluminum surface. There are five layers in Al/B₄C sample and 11 layers in Al/Al₂O₃ with weight fraction of ceramic increasing from 0 in the step of 5%. The microhardness in the FGM specimens is measured at the centers of the individual layers as well as at the interface. The comparison of measured microhardness and that predicted using micromechanics models (rule of mixture, Modified rule of mixture (MROM), and Hopkin-Chamis Method (HCM)) are shown in Fig. 6. The Hardness of 100% Al side of the sample is measured to be 35.725 for Al/Al₂O₃ and 34.35 for Al/B₄C FGM. The hardness of Al₂O₃ and B₄C calculated from hardness of 95/05 portion of the Al/Al₂O₃ and Al/B₄C FGM sample using rule of mixture (ROM), are found to be 115.15 and 135.825, respectively. The hardness of the FGM samples increases with the weight fraction of Al₂O₃ and B₄C as depicted in Fig. 6. It is observed that microhardness increases from 35.72 to 79 from 0 to 50% weight fraction of Al₂O₃ in Al/Al₂O₃ FGM sample whereas for Al/B₄C FGM, microhardness increases from 34.33 to 70.4 for 0 to 20% weight fraction of B₄C. The experimental values of hardness are found to be greater than ROM and closer to MROM (TTO) micromechanics bounds. RROM and equivalent hardness are the farthest from the experimental values. Three measurements taken at center give (X2-X2) higher values of the hardness compared to the one 10 mm away from the ends (X1-X1, X3-X3) due to slight variation in the heat input at the ends compared to center. It is also observed that the applied load during the testing did not produce any sign of cracking.

4. Conclusions

In the paper, the mechanical properties (Young's modulus, Poisson's ratio, Charpy impact energy and hardness) of Al/Al₂O₃ and Al/B₄C composites prepared using powder metallurgy are experimentally measured up to 50% Al₂O₃ and 35% B₄C and compared with the predictions of different micromechanics models. Some of the conclusions drawn from the study are:

- The combination of 600°C temperature, 30 MPa pressure and 1.5 hours duration of sintering leads to samples with 1.93% porosity.
- Young's modulus of Al/Al₂O₃ composite increases from 72 GPa to 119.1 GPa with the increase in Alumina from 0 to 40 % and that of Al/B₄C composite from 72 to 123.2 GPa with the increase in Boron carbide from 0 to 35% with both the composites depicting increase in specific stiffness with the ceramic content.
- The experimental Young's modulus of samples up to 0.40 weight fraction of ceramic are found to lie closely between Ravichandran's/Hashin-Shtrikman lower and Ravichandran's upper bounds, and close to self-consistent/Miller-Lannutti methods based single value predictions for Al/Al₂O₃ and modified rule of mixture, fuzzy logic and self consistent methods predictions for Al/B₄C.
- Experimental Poisson's ratio is found to lie closely between ROM, RLB, RUB, MRUB for Al/Al₂O₃ system and close to ROM, RLB, ZUB, MRUB for Al/B₄C.
- Experimental Charpy energy of samples without notch is found to lie closely between HCM, equivalent Charpy (CEQ) and RLB up to 20 %, and close to RROM for Al/Al₂O₃ weight fraction greater than 20%.
- Rockwell hardness (R_B) of Al/Al₂O₃ increases from 52.66 to 109 for 0 to 50% weight fraction of Al₂O₃ and is found to be close to MROM (TTO) model. Micro-hardness of Al/Al₂O₃ is found to be closer to MROM (TTO) micromechanics.

References

- ASTM Standard C1259 (1998), *Standard Test Method for Dynamic Young's Modulus, Shear Modulus and Poisson's Ratio for Advanced Ceramics by Impulse Excitation of Vibration*, Philadelphia, U.S.A.
- Atri, R.R., Ravichandran, K.S. and Jha, S.K. (1999), "Elastic properties of in-situ processed Ti-TiB composites measured by impulse excitation of vibration", *Mater. Sci. Eng.*, **271**(1), 150-159.
- Budiansky, B. (1965), "On the elastic moduli of some heterogeneous materials", *J. Mech. Phys. Solid.*, **13**(4), 223-227.
- Budiansky, B. (1987), "A new approach to the application of Mori-Tanaka's theory in composite materials", *Mech. Mater.*, **6**(2), 147-157.
- Cannillo, V., Manfredini, T. and Monstorsi, M. (2006), "Microstructure based modeling and experimental investigation in glass-alumina functionally graded materials", *J. Eur. Ceram. Soc.*, **26**(15), 3067-3073.
- Castro, R.R., Wetherhold, R.C. and Kelestemur, M.H. (2002), "Microstructure and mechanical behavior of functionally graded Al A359/SiC composite", *Mater. Sci. Eng.*, **323**(1), 445-456.
- Chegenizadeh, A., Ghadimi B., Nikraz, H. and Simsek, M. (2014), "A novel two-dimensional approach to modeling functionally graded beams resting on a soil medium", *Struct. Eng. Mech.*, **51**(5), 727-741.
- Chmielewski, M., Nosewicz, S., Pietrzak, K., Rojek, J., Strojny, N.A., Mackiewicz, S. and Dutkiewicz, J. (2014), "Sintering behavior and mechanical properties of NiAl, Al₂O₃ and NiAl-Al₂O₃ composites", *J. Mater. Eng. Perform.*, **23**(11), 3875-3886.
- Dalgleish, B.J., Lu, M.C. and Evans, A.G. (1998), "The strength of ceramics bonded with metals", *Acta Metallurg.*, **36**(8), 2029-2035.

- Donnish, V., Reynaud, S. and Haber, R.A. (2011), "Boron carbide: Structure, properties, and stability under stress", *J. Am. Ceram. Soc.*, **94**(11), 3605-3628.
- Ezatpour, H.R., Torabi, P.M. and Sajjadi, S.A. (2013), "Microstructure and mechanical properties of extruded Al/Al₂O₃ composites fabricated by stir-casting process", *Trans. Nonferr. Metals Soc. China*, **23**(5), 1262-1268.
- Gaharwar, V.S. and Umashankar, V. (2014), "The characterization and behavior of Al reinforced with Al₂O₃ fabricated by powder metallurgy", *J. Chem. Technol. Res.*, **6**(6), 3272-3275.
- Gibson, R.F. (1994), *Principles of Composite Materials Mechanics*, McGraw-Hill, New York, U.S.A.
- Hashin, Z. and Shtrikman, S. (1963), "A variational approach to the theory of the elastic behaviour of multiphase materials", *J. Mech. Phys. Solid.*, **11**(2), 127-140.
- Hill, R. (1965), "A self-consistent mechanics of composite materials", *J. Mech. Phys. Solid.*, **13**(4), 213-222.
- Hirano, T., Teraki, J. and Yamanda, T. (1991), "Application of fuzzy theory to the design of functionally gradient materials", *Proceedings of the 11th International Conference on Structural Mechanics in Reactor Technology*, Tokyo, Japan, August.
- Hirano, T., Teraki, J., and Yamanda, T. (1990), "On the design of functionally gradient materials", *Proceedings of the 1st International Symposium on Functionally Gradient Materials*, Sendai, Japan.
- Hsieh, C.L. and Tuan, W.H. (2005), "Elastic properties of ceramic-metal particulate composites", *Mater. Sci. Eng.*, **393**(1), 133-139.
- Hsieh, C.L. and Tuan, W.H. (2005), "Poisson's ratio of two-phase composites", *Mater. Sci. Eng.*, **396**(1), 202-205.
- Hsieh, C.L. and Tuan, W.H. (2006), "Elastic and thermal expansion behavior of two-phase composites", *Mater. Sci. Eng.*, **425**(1), 349-360.
- Hsieh, C.L., Tuan, W.H. and Wu, T.T. (2004), "Elastic behavior of a model two-phase material", *J. Eur. Ceram. Soc.*, **24**, 3789-3793.
- Joseph, R.Z. (1995), "Functionally graded materials: Choice of micromechanics model and limitations in property variation", *Compos. Eng.*, **5**(7), 807-819.
- Kapurja, S., Bhattacharyya, M. and Kumar, A.N. (2008), "Theoretical modeling and experimental validation of thermal response of metal-ceramic functionally graded beams", *J. Therm. Stresses*, **31**(8), 759-787.
- Kerner, E.H. (1956), "The elastic and thermo elastic properties of composite media", *Proceedings of the Physical Society*, **69**(8), 808-813.
- Kim, J. and Muliana, A. (2010), "Time-dependent and inelastic behaviours of fiber- and particle hybrid composites", *Struct. Eng. Mech.*, **34**(4), 525-539.
- Kothari, K., Radhakrishnan, R., Sudarshan, T.S. and Wereley, N.M. (2012), "Characterization of rapidly consolidated Y-TiAl", *Adv. Mater. Res.*, **1**, 51-74.
- Mahendran, G., Balasubramaniam, V. and Senthilvelan, T. (2012), "Mechanical and metallurgical properties of diffusion bonded AA2024 Al and AZ31B Mg", *Adv. Mater. Res.*, **1**(2), 147-160.
- Miller, D.P., Lannutti, J.J. and Noebe, R.D. (1993), "Fabrication and properties of functionally graded NiAl/Al₂O₃ composite", *J. Mater. Res.*, **8**(8), 2004-2013.
- Mori, T. and Tanaka, K. (1973), "Average stress in matrix and average elastic energy of materials with misfitting inclusions", *Acta Metallurg.*, **21**(5), 571-574.
- Nan, C.W., Yuan, R.Z. and Zhang, L.M. (1993), "The physics of metals/ceramics functionally gradient materials", *Ceram. Trans. Am. Ceram. Soc. Westerv.OH*, **34**, 75-82.
- Prabhu, T.N., Demappa, T., Harish, V. and Prashantha, K. (2015), "Synergistic effect of clay and polypropylene short fibers in epoxy based terminal composite hybrids", *Adv. Mater. Res.*, **4**(2), 97-111.
- Ravichandran, K.S. (1994), "Elastic properties of two phase composites", *J. Am. Ceram. Soc.*, **77**(5), 1178-1184.
- Rousseau, C.E. and Tippur, H.V. (2002), "Evaluation of crack tip fields and stress intensity factors in functionally graded elastic materials: cracks parallel to elastic gradient", *J. Fract.*, **114**(1), 87-112.
- Sajjadi, S.A., Ezatpour, H.R. and Torabi, P.M. (2012), "Comparison of microstructure and mechanical properties of A356 aluminium alloy/Al₂O₃ composites fabricated by stir and compo-casting processes", *Mater. Des.*, **34**, 106-111.

- Sasaki, M., Wang, Y. and Hirano, T. (1989), "Design of SiC/C functionally gradient materials and its preparation by chemical vapor deposition", *J. Ceram. Soc.*, **97**(5), 539-534.
- Srivatsan, T.S., Manigandan, K., Godbole, C., Paramsothy, M. and Gupta, M. (2012), "The tensile deformation and fracture behavior of a magnesium alloy nanocomposite reinforced with nickel", *Adv. Mater. Res.*, **1**(3), 169-182.
- Tamura, I., Tomata, Y. and Ozawa, H. (1973), "Strength and ductility of Fe-Ni-C alloys composed of austenite and martensite with various strengths", *Proceedings of the 3rd International Conference of Strength of Materials and Alloys*, Cambridge, U.K., August.
- Tilbrook, M.T., Moon, R.J. and Hoffman, M. (2005), "On the mechanical properties of alumina-epoxy with interpenetrating network structure", *Mater. Sci. Eng.*, **399**(1-2), 170-178.
- Upadhyay, A., Beniwal, R.S. and Singh, R. (2012), "Elastic properties of Al₂O₃-NiAl: A modified version of Hashin-Shtrikman bounds", *Continuum. Mech. Thermodyn.*, **24**(1), 257-266.
- Voigt, W. (1989), "Über die beziehung zwischen den beiden elastizitätskonstanten isotroper körper", *Wied. Ann.*, **38**, 573-587.
- Wakashima, K. and Tsukamoto, H. (1990), "Micromechanical approach to the thermo mechanics of ceramic-metal gradient material", *Proceedings of the 1st International Symposium on Functionally Gradient Materials*, The Functionally Graded Forum Series, Japan.
- Zimmerman, R.W. (1992), "Hashin-Shtrikman bounds on the poisson's ratio of composite materials", *Mech. Res. Commun.*, **19**(6), 563-569.

CC

Abbreviations

CEQ	Charpy Energy Equivalent
CPA	Coherent Potential Approximation
FGM	Functionally Graded Material
FLM	Fuzzy Logic Method
HCM	Hopkin-Chamis Method
HEQ	Hardness Equivalent
HSLB/HSUB	Hashin-Shtrikman Lower/Upper Bounds
HTM	Halpin-Tsai Method
MLM	Miller and Lannutti Method
KM	Kerner Method
MRLB/MRUB	Modified Ravichandran Lower/Upper Bounds
MROM	Modified Rule of Mixture
MTM	Mori-Tanaka Method
RLB/RUB	Ravichandran Lower/Upper Bounds
ROM/ RROM	Rule of Mixture/Reciprocal Rule of Mixture
SCM	Self-consistent Method
TTO	Tomura, Tomoto and Ozara Model
WTM	Wakashima and Tsukamoto Method
ZLB/ ZUB	Zimmerman Lower/Upper Bounds

